Molecular Architecture of Electroactive and Biodegradable Copolymers Composed of Polylactide and Carboxyl-Capped Aniline Trimer

Baolin Guo, Anna Finne-Wistrand, and Ann-Christine Albertsson*

Department of Fibre and Polymer Technology, School of Chemical Science and Engineering, Royal Institute of Technology, SE-100 44, Stockholm, Sweden

Received October 2, 2009; Revised Manuscript Received January 27, 2010

Two-, four-, and six-armed branched copolymers with electroactive and biodegradable properties were synthesized by coupling reactions between poly(L-lactides) (PLLAs) with different architecture and carboxyl-capped aniline trimer (CCAT). The aniline oligomer CCAT was prepared from amino-capped aniline trimer and succinic anhydride. FT-IR, NMR, and SEC analyses confirmed the structure of the branched copolymers. UV−vis spectra and cyclic voltammetry of CCAT and copolymer solution showed good electroactive properties, similar to those of polyaniline. The water contact angle of the PLLAs was the highest, followed by the undoped copolymer and the doped copolymers. The values of doped four-armed copolymers were 54−63°. Thermal properties of the polymers were studied by DSC and TGA. The copolymers had better thermal stability than the pure PLLAs, and the T_g between 48−58 °C and T_m between 146−177 °C of the copolymers were lower than those of the pure PLLA counterparts. This kind of electroactive and biodegradable copolymer has a great potential for applications in cardiovascular or neuronal tissue engineering.

Introduction

Research on conductive polymers for biomedical applications expanded greatly with the discovery that these materials were compatible with many biological molecules.[1,2] Recent studies have also shown that electrical signals can regulate cellular activities, including DNA synthesis, cell adhesion, migration, proliferation, and differentiation.[3,4] Considerable interest has been shown in conducting polymers and their derivatives, such as polypyrrole,[3,5] polyaniline,[6,7] polythiophene,[8] and polyethylenedioxythiophene.[9] For example, Hodgson[10] assessed different oxidation states of polyaniline in vivo, and no obvious inflammation was found. Langer[3] showed with a culture of the NGF-induced rat neuronal pheochromocytoma cells (PC-12) that polypyrrole greatly enhanced the neurite outgrowth and spreading of PC-12 cells.

Blends, composites, block copolymers, or graft copolymers have been prepared from polyaniline, polypyrrole, and polymers such as heparin,[11] chitosan,[12,13] collagen,[6,14] poly (ethylene glycol),[15] polylactide,[16,17] and oligopeptides,[18,19] which were found more suitable in tissue engineering. However, there are practical problems when these conductive polymers are used in tissue engineering. The main drawbacks of the existing system are poor polymer−cell interaction, absence of a cell interaction site, hydrophobicity, poor solubility and processability, and uncontrollable mechanical properties.[4] One of the biggest limitations for in vivo applications in tissue engineering of conductive polymers is their inherent inability to degrade, so that the incorporation of conducting polymers into biodegradable polymer to obtain materials with both electroactive and biodegradable properties is still a challenge. Langer et al.[20] prepared erodible conducting polymers based on β-substituted pyrrole monomers containing ionizable and/or hydrolyzable side groups. Schmidt et al.[21] synthesized polymers from conducting oligomers of pyrrole and thiophenes which were connected together via degradable ester linkages and then concluded that this polymer was conductive, degradable, and biocompatible. Recently, Schmidt et al.[22] incorporated alternating electroactive quaterthiophene units and biodegradable ester units into one macromolecule; they demonstrated that the copolymer was biodegradable and electroactive and that the copolymer was nontoxic to Schwann cells in vitro. Zhang et al.[16] obtained electrically conductive biodegradable composite from polypyrrole nanoparticles and poly(D,L-lactide). Wei et al.[23] incorporated aniline pentamer (AP) into polylactide and obtained linear triblock copolymers that showed good electroactive, biodegradable, and processing properties, but poor mechanical properties because of their low molecular weights. Wei and co-workers[24] later synthesized linear multiblock copolymers of polylactide and AP with higher molecular weights, which were electroactive and biodegradable and which could accelerate the differentiation of PC-12 cells. Zhang et al.[25] synthesized linear degradable electrically conducting copolymers of AP and polyglycolide. Amino-capped aniline trimer (ACAT) has a well-defined electroactive structure, good processing properties, and ease of degradability.[26,27] It exhibits electronic and optical properties that are remarkably similar to those of polyaniline.[28,29] We have therefore incorporated the electroactive aniline trimer into PLLAs to obtain biodegradable and electroactive copolymers in this paper.

Our group has worked on the synthesis of (co)polymers from lactones for many years, and we have synthesized many (co)polymers with different architectures.[30–35] Architecture plays an important role on the performance of polymers. Lately, star-shaped homo- and copolymers have been shown to be an interesting alternative to their linear analogues in their interaction with surrounding tissue. As a result, we used branched PLLAs to couple with CCAT to obtain star-shaped electroactive and biodegrable copolymers, which will have a better interaction with the tissue. First, an electroactive CCAT was synthesized

* To whom correspondence should be addressed. Tel.: +46-8-790 8274. Fax: +46-8-20 84 77. E-mail: aila@polymer.kth.se.

10.1021/bm9011248
Published on Web 03/04/2010

Scheme 1. Schematic Synthesis of Carboxyl-Capped Aniline Trimer and the Copolymers

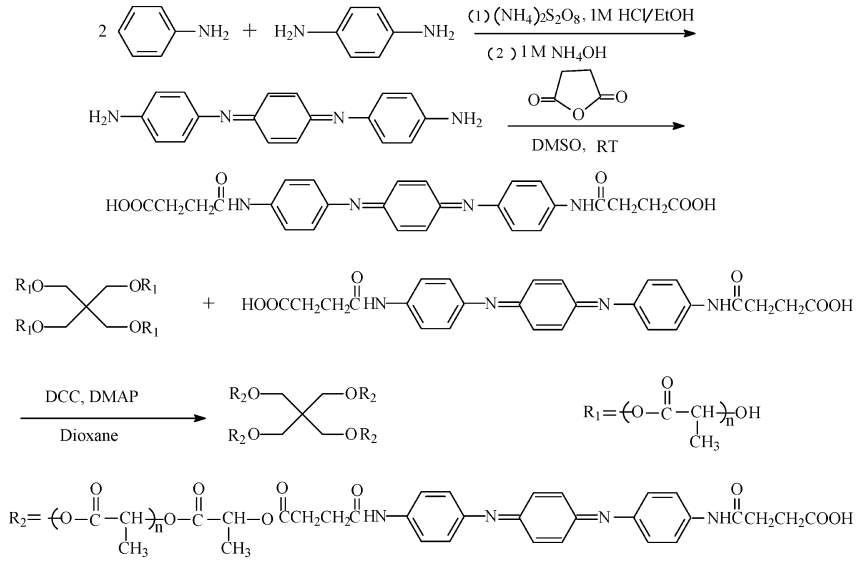

from ACAT, and characterized, then coupled with linear, four- and six-armed star-shaped hydroxyl-capped polylactides to generate a series of electroactive and biodegradable copolymers with different architectures. Degradable polymers with different architectures are used in tissue engineering and the architectural design is a valuable tool for tuning the mechanical properties. We hypothesize that, by adding electroactive properties to these polymers, we obtain an additional parameter that can be utilized for optimal cell culturing results.

Experimental Section

Materials. L-Lactide (LLA; Aldrich) was purified by recrystallization in dry toluene and subsequently dried under reduced pressure (10^{-2} mbar) at room temperature for at least 48 h prior to polymerization. Toluene (Lab-Scan, 99.8%) was dried over a Na wire before use. Aniline (Aldrich) was distilled twice under reduced pressure. Stannous octoate, $Sn(Oct)_2$ (Aldrich), was dried over molecular sieves and kept under an inert atmosphere before use. *p*-Phenylenediamine, ammonium persulfate ($(NH_4)_2S_2O_8$), ammonium hydroxide (NH_3OH), hydrochloric acid (HCl), ethanol (EtOH), dimethyl sulphoxide (DMSO), succinic anhydride (SA), chloroform ($CHCl_3$), hexane, methanol, 1,4-dioxane, *N*,*N*′-dicyclohexyl carbodiimide (DCC), 4-dimethylaminopyridine (DMAP), and camphorsulfonic acid (CSA) were all purchased from Aldrich and were used as received.

Synthesis of Carboxyl-Capped Aniline Trimer. ACAT was synthesized according to previous reports.[36] Briefly, ACAT was obtained by oxidative coupling of *p*-phenylenediamine and 2 equiv amounts of aniline with equivalent amounts of $(NH_4)_2S_2O_8$ as oxidant, as shown in Scheme 1. ^{1}H NMR (400 MHz, DMSO-d_6) δ 6.96 (s, 4H, Ar−H), 6.81 (d, 4H, Ar−H), 6.62 (d, 4H, Ar−H), 5.43 (s, 4H, -NH_2). ^{13}C NMR (100 MHz, DMSO-d_6) δ 155.21 (Ar−C), 147.69 (Ar−C), 139.35 (Ar−C), 135.18 (Ar−C), 124.33 (Ar−C), 114.13 (Ar−C). This result agrees well with ref 36.

For the synthesis of CCAT, ACAT (0.2280 g, 0.001 mol), and SA (0.3000 g, 0.003 mol) were added into a dry flask with magnetic stirrer, and 15 mL of dry DMSO was then poured into the flask and the flask was sealed. After a reaction for 24 h at room temperature, the solution was dropped into 300 mL of distilled water and then precipitated in HCl solution, pH = 1. The precipitate was collected by filtration and washed thoroughly with distilled water. Finally, the product was dried in a vacuum oven at room temperature for 48 h. Characterization: ^{1}H NMR (400 MHz, DMSO-d_6) δ 10.05 (s, 2H, −COOH), 9.70 (s, 2H, -NHCO-), 7.63 (d, 4H, Ar−H), 7.38 (s, 4H, Ar−H), 6.87 (d, 4H, Ar−H). ^{13}C NMR (100 MHz, DMSO-d_6) δ 174.14 (-COOH), 170.30 (-NHCO-), 157.74 (Ar−C), 145.04 (Ar−C), 137.21 (Ar−C), 125.15 (Ar−C), 121.89 (Ar−C), 119.66 (Ar−C), 31.25 (-CH_2-), 29.03 (-CH_2-). The synthetic route is shown in Scheme 1.

Synthesis of Branched PLLAs. Branched PLLA was prepared by ring-opening polymerization[32] (ROP) as follows: a silanized round-bottomed flask was used as the reactor. The monomer (LLA), initiator ($Sn(Oct)_2$), and co-initiator (ethylene glycol (EG), pentaerythritol (Pen), and inositol (Ino)) were weighed and added into the flask in a glovebox (Mbraun MB 150B-G-I) purged with nitrogen. The mixture was then immersed in an oil bath at 110 °C under a nitrogen atmosphere for an appropriate time. The theoretical molecular weights of each kind of PLLA were set to 80000, 40000, and 20000, respectively. After reaction, 10 mL of chloroform was added in the flask to dissolve the mixture, which was then precipitated in 300 mL of hexane/methanol (v/v = 95:5) solution. After filtration, the product was dried in a vacuum oven at room temperature for 24 h. Samples were coded as, for example, EG-PLLA80000, which denoted a PLLA initiated by ethylene glycol for which the theoretical molecular weight was 80000.

Synthesis of the Copolymers. The schematic routine for the synthesis of copolymer with four-armed PLLA and CCAT as an example is shown in Scheme 1. Purified Pen-PLLA40000 (0.436 g, 1.5×10^{-5} mol) and CCAT (0.03 g, 6×10^{-5} mol) were dissolved in 10 mL of 1,4-dioxane in a flame-dried flask with a magnetic stirrer, and DMAP (0.017 g, 1.5×10^{-4} mol) and DCC (0.034 g, 1.5×10^{-4} mol) were then added into the flask. The reaction was kept at 0 °C for 48 h. After the reaction, the mixture was filtered to remove dicyclohexylurea. The filtrate was precipitated in a mixture of hexane and methanol (vol. (hexane)/vol. (methanol) = 95:5). The product obtained was dried in a vacuum oven for 48 h after filtration.

Characterization. FT-IR spectra of ACAT, CCAT, PLAAs, and the copolymers were recorded on a "Perkin Elmer Spectrum 2000" spectrometer (Perkin-Elmer Instrument, Inc.). Each spectrum was taken as the average of 20 scans at a resolution of 4 cm^{-1}.

^{1}H and ^{13}C NMR spectra were recorded on a Bruker Avance 400 and 100 MHz NMR instruments, $CDCl_3$ being used as the solvent for all the PLLAs samples and as internal standard (δ = 7.26 and 77.0 ppm). For aniline trimer and copolymer, DMSO-d_6 was used as the solvent at room temperature and as internal standard (δ = 2.50 and 39.5 ppm).

Number of average molecular weight, molecular weight distribution (M_w/M_n) values, and α-parameter from Mark−Houwink equation of polymers were determined by GPC experiments conducted in chloroform at 40 °C at a flow rate of 1 mL/min using a Spectra-Physics 8800 solvent delivery system with a set of two PLgel 5 μm MIXED-C ultrahigh efficiency column, a Shodex SE 61 refractive index detector,

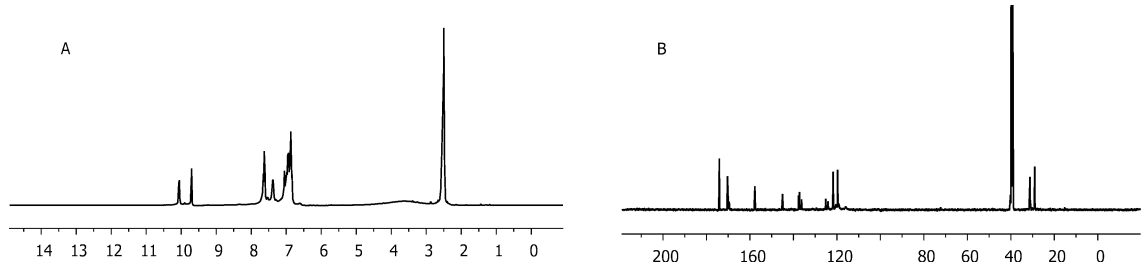

Figure 1. ^{1}H (A) and ^{13}C NMR (B) spectra of carboxyl-capped aniline trimer.

and a viscometer. Polystyrene standards with narrow molecular weight distributions were used as calibration.

The UV−vis spectra of ACAT, CCAT, and copolymer solutions were monitored on a UV−vis spectrophotometer (UV-2401).

Glass transition temperature (T_g) and melting temperature (T_m) were measured by differential scanning calorimetry (DSC) using a Mettler-Toledo DSC 820 module under a nitrogen atmosphere (nitrogen flow rate of 80 mL/min). Measurements were made during the first heating scan from −20 to 200 °C, the first cooling from 200 to −20 °C, and the second heating scan from −20 to 200 at 10 °C /min. Data for T_m and T_g were taken from the second heating scan.

The thermal stability of the PLLAs and copolymers was estimated by thermogravimetric analysis (TGA) under a nitrogen atmosphere (nitrogen flow rate 50 mL/min) with a sample mass of 10 ± 1 mg and a heating rate of 10 °C/min. The scan range was from 30 to 800 °C.

Cyclic voltammetry (CV) of aniline trimer and copolymers was performed on an Electrochemical Workstation interfaced and monitored with a PC computer. A three-electrode system was employed, consisting of a platinum disk working electrode (surface area 0.14 cm^2), a platinum-wire auxiliary electrode, and a reference electrode. The reference electrodes used were Ag/AgCl for DMSO/H_2O mixture. All the solutions were deoxygenated for 10 min with nitrogen prior to the electrochemical measurements. The scan rate used was 60 mV/s.

Water contact angle measurements of the copolymer films were measured using a contact angle and surface tension meter (KSV instruments Ltd.). A drop of Milli-Q water was placed on the surface of the sample and the images of the water menisci were recorded by a digital camera. The KSV software was used to analyze the images and gave the contact angle data. The contact angle of each sample was taken as the average of five measurements at different points.

Results and Discussion

Synthesis of Carboxyl-Capped Aniline Trimer. The structure of CCAT was confirmed by NMR as shown in Figure 1. The fact that there is no peak arising from the amino group (δ = 5.4 ppm) in Figure 1A demonstrates that ACAT is completely changed into CCAT. There are small peaks around 137 and 125 ppm in the ^{13}C NMR spectrum in Figure 1B because CCAT is in an emeraldine state and the NMR spectrum is affected by the quinoid signals.[23] CCAT contains carboxyl groups at both end of the monomer, so it can be introduced into polymer by graft or copolymerization, and the hydrophilicity should also increase because of the introduction of carboxyl groups into CCAT.

Synthesis of Branched PLLAs. Linear, four- and six-armed PLLAs with different molecular weights were synthesized by ROP. $Sn(Oct)_2$ was used as initiator, and the ratio of monomer to initiator was 10000:1. The organic metal residuals in the PLLA are therefore very low, and the polymers can thus be used in tissue engineering.[37]

Figure 2B shows the ^{1}H NMR of Pen-PLLA40000. No peak is observed between 3.0 and 4.0 ppm corresponding to nonreacted hydroxyl groups of pentaerythritol, and this means that the number of molecular branches should be the same as the number of the hydroxyl groups of the pentaerythritol. In addition, the $-CH_2-$ (δ = 4.3 ppm) of the pentaerythritol appears in the ^{1}H NMR spectra (Figure 2B), which is also confirmed in the ^{13}C NMR spectra of Pen-PLLA40000 (Figure 2D), the signal of pentaerythritol appearing at 66.9 ppm. Thus, Pen-PLLA40000 with a four-armed branched structure is certainly obtained. The hydroxyl group (δ = 2.7 ppm) at the PLLA chain end is also seen in the ^{1}H NMR spectra. This will be used for the coupling of the hydroxyl-capped PLLA and CCAT in the next step. The same trends are found in the EG and Ino systems.

Monomer conversion of the sample was determined by ^{1}H NMR by comparing the peak integrals of methine protons of PLLA (δ = 5.2 ppm in Figure 2) with those of lactide (δ = 5.0 ppm in Figure 2), and the results are summarized in Table 1. The conversion of Ino as co-initiator is lower, but it exceeds 86% after 4 days of reaction. The monomer conversions of the other co-initiators system are all higher than 92%, which indicates that the low concentration of $Sn(Oct)_2$ has good catalyst activity.

Molecular weights of the PLLA segment were calculated by comparing the peak integrals of methine protons (δ = 5.2 ppm, CH in Figure 2) with those of the methine protons next to the terminal hydroxyl groups (δ = 4.4 ppm, CH (end) in Figure 2). The PLLA segment was equivalent to the PLLA molecular chains of each branch; that is, the $M_{n\text{-NMR}}$ of the PLLA segment denoted the number average molecular weight of each branch. The molecular weights calculated by NMR are also listed in Table 1. We found that the molecular weight increase with the increase of the ratio of the monomer to co-initiator. The molecular weight determined by NMR was very close to the GPC results as shown in Table 1, and the molecular weight distribution was quite narrow. The relationship between intrinsic viscosity and molecular weight was analyzed by the Mark−Houwink equation $[\eta] = kM^{\alpha}$; the values of α is 0.5 at the theta state and is in the range of 0.65−0.8 for linear random coils in the good solvent. It is found that the α of the six- and four-armed polymers are smaller than the linear counterparts with the similar molecular weight, which indicates a smaller hydrodynamic size and a more compact structure of the branched polymers. These results further confirm the star-shaped structures of the polymers. It is observed that some of the molecular weights are not in accordance with the theoretical ones. This is because the $Sn(Oct)_2$ catalyzes transesterification reactions and the conversion did not reach 100%, as shown in Table 1.

Characterization of the Copolymers. Copolymers were characterized by FT-IR and NMR. Figure 3 shows the IR spectra of the copolymer together with those of its corresponding precursors. Curves a, b, c, and d are the IR spectra of ACAT, CCAT, Pen-PLLA20000, and Copo-Pen-PLLA20000, respectively. In Figure 3a, the characteristic absorption bands at 3308

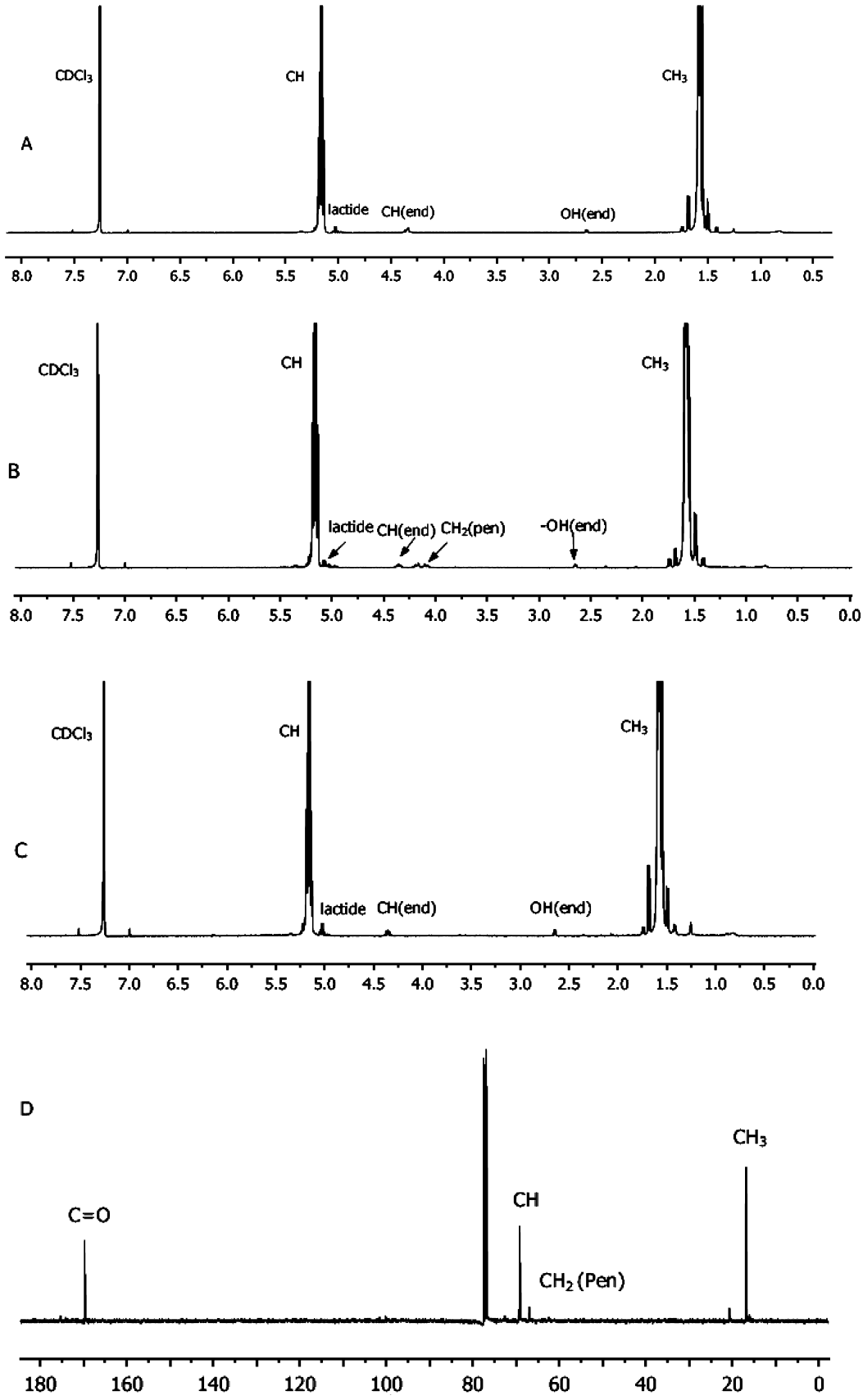

Figure 2. ^{1}H NMR spectra of EG-PLLA40000 (A), Pen-PLLA40000 (B), Ino-PLLA40000 (C), and ^{13}C NMR spectrum of Pen-PLLA40000 (D).

and 3201 cm^{-1} arising from the terminal $-NH_2$ of ACAT are observed. The characteristic peaks at 1597 and 1499 cm^{-1} are assigned to the stretching vibrational bands of quinoid rings and benzenoid rings, respectively. Compared to curve a, the new peak at 3246 cm^{-1} and peaks at 1722 and 1660 cm^{-1} corresponding to carbonyl groups ($-CO-$) in the $-COOH$ and $-NHCO-$ groups reveal that the aromatic amine $-NH_2$ in the ACAT was successfully converted into the imine $-NHCO-$.

Table 1. Properties of Branched PLLAs

sample code	reaction time (h)	monomer conversion (%)	molecular weight determined by NMR	molecular weight determined by GPC (M_w/M_n)	α from Mark−Houwink equation
EG-PLLA80000	72	92	58000	67200 (1.17)	0.63
EG-PLLA40000	72	94	32200	30000 (1.37)	0.68
EG-PLLA20000	72	99	14700	18530 (1.29)	0.73
Pen-PLLA80000	48	97	59800	50050 (1.12)	0.50
Pen-PLLA40000	72	97	29100	20200 (1.15)	0.53
Pen-PLLA20000	72	97	14700	11230 (1.31)	0.54
Ino-PLLA80000	96	86	43600	40800 (1.12)	0.45
Ino-PLLA40000	72	97	42900	34000 (1.21)	0.47
Ino-PLLA20000	72	98	22000	21600 (1.30)	0.55

Due to the electron-withdrawing group at both ends of CCAT, the characteristic absorption band of the quinoid unit shift to 1575 cm^{-1} is shown in Figure 3b. The peaks at 3308 and 3201 cm^{-1} corresponding to $-NH_2$ of ACAT have completely disappeared (Figure 3b), which confirms the total transformation from ACAT to CCAT. Compared with curves b and c, curve d contains peaks at 1670, 1593, and 1496 cm^{-1} from the CCAT segment, and peaks at 1748, 1180, and 1078 cm^{-1} assigned to −CO− and C−O−C groups from the Pen-PLLA segment. All these data demonstrate that the copolymer was obtained. Curve d also shows a small peak at 3498 cm^{-1} arising from the −OH groups at the end of the copolymer, which are very important in tissue engineering, because they increase the hydrophilicity of materials and improve cell adhesion to the copolymers.

To further confirm the structure of the copolymer, the copolymer was characterized by ^1H NMR in DMSO-d_6, and the result of the Copo-Pen-PLLA20000 copolymer is shown in Figure 4 (see Supporting Information for the two- and six-armed copolymer). Copo-Pen-PLLA20000: ^1H NMR (400 MHz, DMSO-d_6) δ 10.07 (s, 1H, -COOH), 9.71 (s, 2H, -NHCO-), 7.63 (d, 4H, Ar−H), 7.34 (d, 4H, Ar−H), 6.94 (d, 4H, Ar−H), 2.62 (t, 2H, -CH_2CH_2-) for the CCAT segment, and 5.19 (t, 2H, poly -CH), 4.24 (s, 2H, Pen), 1.45 (d, 3H, poly), 1.27 (d, 3H) for the Pen-PLLA segment. The chemical shift of the end chain CH group in the pure PLLAs is around 4.4 ppm, and it was shifted to around 4 ppm in the copolymer as a result of the coupling reaction of the hydroxyl groups at the PPLA chain end and the carboxyl groups of CCAT, which confirms the successful esterification in the copolymer.

In addition, two solubility tests demonstrated the successful synthesis of the copolymer. CCAT dissolves easily in 1 mol/L NaOH solution (red solution), but the copolymer did not dissolve in the NaOH solution (colorless solution). CCAT does not dissolve in $CHCl_3$ (colorless solution), but the copolymers dissolved in $CHCl_3$ easily (light red solution). All these phenomena and data demonstrate that the copolymer was successfully obtained. The good solubility of the copolymer in $CHCl_3$ also provides a convenient processing property of the copolymer.

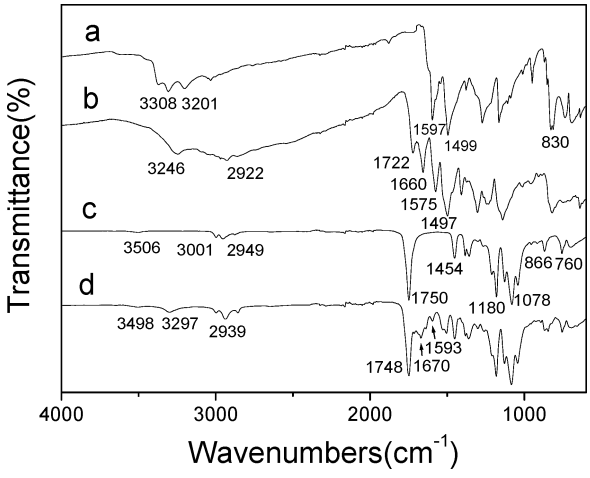

Figure 3. FT-IR spectra of ACAT (a), CCAT (b), Pen-PLLA20000 (c), and Copo-Pen-PLLA20000 (d).

Electroactive Properties of ACAT, CCAT, and Copolymers. Electrochemical properties of the monomer and copolymers were studied by UV−vis spectra and cyclic voltammetry.

The UV−vis spectra of ACAT, CCAT, and copolymers in DMSO solution are shown in Figure 5. The UV absorption spectra (Figure 5a,b) of ACAT and CCAT show a typical broad quinoid absorption peak at about 520 nm (CCAT) and 590 nm (ACAT), and a narrower benzenoid peak at about 330−340 nm. The quinoid peak is related to the excitonic transition of $\pi b-\pi q$ from the benzene unit to the quinone unit, while the benzenoid peak is attributed to the $\pi-\pi^*$ transition in the benzene unit, which is similar to that of polyaniline.[38] The quinoid/benzenoid intensity ratio decreases together with a slight blue shift caused by enhanced conjugation arising from covalent modification by imine groups that facilitates the delocalization of electrons in the benzene unit, as shown in Scheme 2. Consequently, the electronic concentration of quinone units is reduced, and the intensity of the $\pi b-\pi q$ transition is decreased. There is no new absorption as a result of the synthesis of CCAT and copolymers, and this indicates that the ACAT in the CCAT and copolymers remains in the emeraldine base form.

In Figure 5, it is evident that the UV−visible absorption spectra of all the copolymers are similar to that of CCAT, although the intensity of the UV absorbance decreases with increasing molecular weight of the Pen-PLLA segment, that is, with decreasing the CCAT content in the copolymer. There is no obvious blue shift in Figure 5c−e. This is different from previously reported data,[23] in which the leucoemeraldine polylactide-AP triblock copolymers in DMF solutions have a shift that increases with decreasing AP content in the copolymer, because the incorporation of the long and flexible PLA chains into the triblock copolymer may restrict the planar conformation of AP backbone in the copolymers, leading to decrease in the effective conjugation length of the AP. We prepared the CCAT segment at the end of the copolymer chain, so the copolymers chains have little effect on the conjugation length of the CCAT segment, which can retain its good electroactive properties.

Figure 6 shows the UV−visible spectra of Copo-Pen-PLLA20000 in different solutions. The absorption peaks in $CHCl_3$ and 1,4-dioxane are somewhat lower, and there is a blue shift compared to the peak in DMSO solution (Figure 6a). This is related to the polarity of the solvents. A decrease in polarity of the solvent leads to a blue shift of the absorbance peak. A

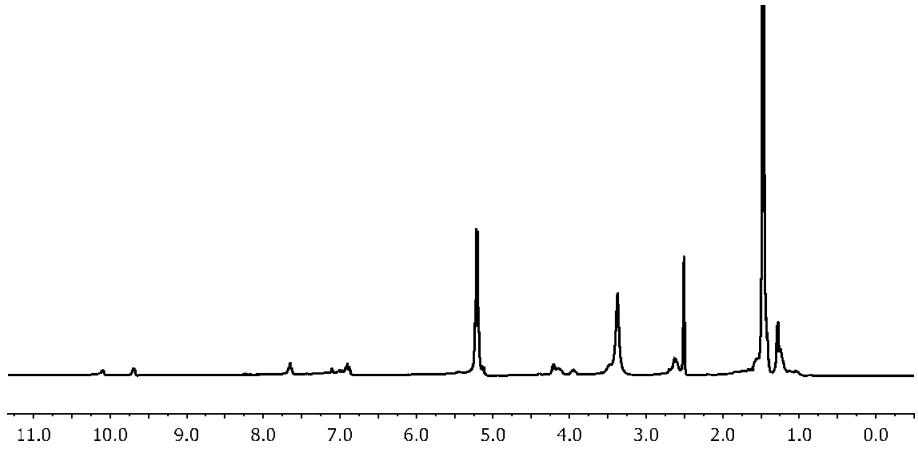

Figure 4. ^{1}H NMR of the Copo-Pen-PLLA20000 copolymer.

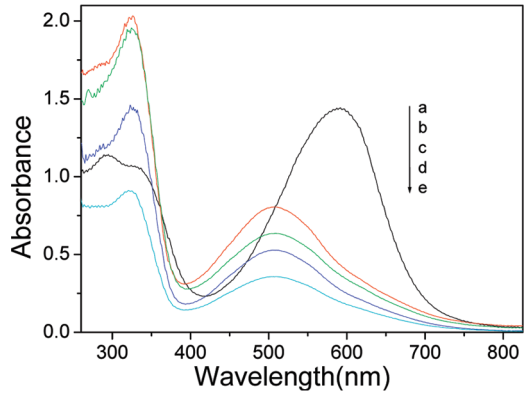

Figure 5. UV spectra of ACAT (a), CCAT (b), Copo-Pen-PLLA20000 (c), Copo-Pen-PLLA40000 (d), and Copo-Pen-PLLA80000 (e).

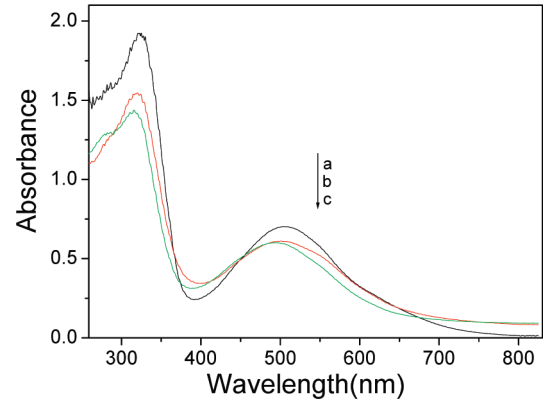

Figure 6. UV spectra of Copo-Pen-PLLA20000 in different solvents at the same concentration: solvent a, DMSO; b, 1,4-dioxane; c, $CHCl_3$.

second reason is that the solubility of CCAT segment in $CHCl_3$ remains poor although the solubility of the copolymers in $CHCl_3$ is greatly improved because of the PLLA segments. Good solubility of PLLA segments in the copolymer in $CHCl_3$ will force the CCAT segment to disperse in $CHCl_3$. This pseudo-solubility is confirmed by the ^{1}H NMR spectrum of the copolymer in $CDCl_3$, in which there were no signals from the CCAT segment.

We also studied the effect of the amount of dopant (HCl) on the UV spectra of Copo-Pen-PLLA20000. In order to keep the concentration of the copolymer constant in the solution, 4 mol/L HCl was continuously added to the sample vial. The change in the UV spectra of the copolymer solution is plotted in Figure 7. Figure 7 shows that two characteristic peaks at 330 and 520 nm corresponding to the benzene and quinoid gradually disappear with increasing the doped ratio (curves a→g) and that three new peaks appear at 415, 638, and 818 nm, which are related to the formation of polarons from the electron transition of quinoid to benzenoid units (see Scheme 2). In Figure 7, the peak at 638 nm increases with increasing doped ratio from 1:5 to 1:300 (curve e) and then begins to decrease with increasing the doped ratio. This may be because the excess of HCl in the solution will impair the hyperfine structure of the complex of

Scheme 2. Proposed Mechanism[39] for the HCl Doping of the Copo-Pen-PLLA20000

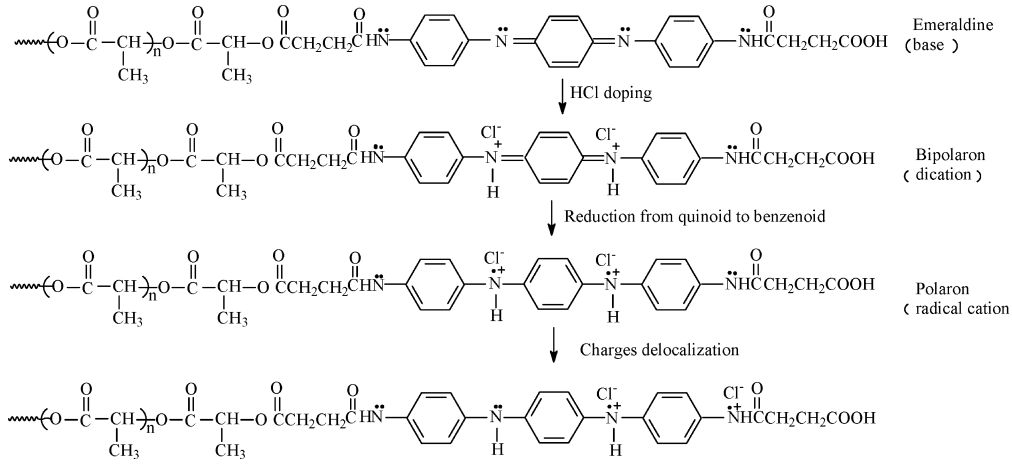

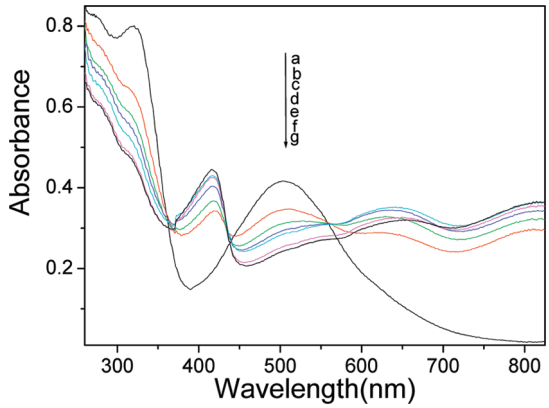

Figure 7. UV spectra of doping process of Copo-Pen-PLLA20000 with HCl, (a) undoped copolymer, (b) doping ratio 1:5, (c) 1:10, (d) 1:100, (e) 1:300, (f) 1:1000, and (g) 1:4000.

aniline trimer radical cations paired with counterions and cause the aggregates that form the bipolaron intermediates to dissociate at the same time.[39]

Figure 8 shows cyclic voltammetry data for (a) ACAT, (b) CCAT, and (c) representative Copo-Pen-PLLA20000 obtained in a DMSO/HCl aqueous solution mixture. The Vol. (1 M HCl)/Vol. (DMSO) ratio was 1:1, and the concentration 0.0125% w/w for ACAT and CCAT, and Vol. (1 M HCl)/Vol. (DMSO) ratio was 1:7 and the concentration 0.00625% w/w for Copo-Pen-PLLA20000. The copolymer cannot be tested at a higher HCl/DMSO ratio because the copolymer precipitates in the high HCl concentration solution. Under these conditions, the cyclic voltammogram for ACAT (Figure 8a) showed two pairs of redox peaks, similar to those of polyaniline.[40] The first pair of the well-defined redox peaks at 0.54 V can be attributed to the reversible redox process from the "leucoemeraldine" to the "emeraldine" form (Scheme 3). At higher potentials, a reversible redox peak at 0.70 V is assigned to the oxidation/reduction of the "emeraldine" form to the "pernigraniline" state. The cyclic voltammogram for CCAT (Figure 8b) is similar to that for ACAT, but the oxidization is higher than that of ACAT. This is because the electron withdrawing imine group in CCAT decreases the electron concentration of CCAT, so that it needs higher voltage to oxidize. The cyclic voltammogram of Copo-Pen-PLLA20000 (Figure 8c) also shows two pairs of peaks at 0.42 and 0.60 V, which are assigned to the transition from the leucoemeraldine oxidation state to the emeraldine oxidation state and then to the "pernigraniline" state (Scheme 3). The oxidization peaks of the copolymer are somewhat lower than those of CCAT. This is attributed to the different test condition such as different HCl and copolymer concentrations.[26] All these spectroscopic and electrochemical results demonstrate the good electroactivity of the copolymers (see Supporting Information for CVs of Copo-EG-PLLA20000 and Copo-Ino-PLLA20000).

Water Contact Angle of the Polymers. It is known that the surface hydrophilicity is an important feature of polymeric biomaterials. Surfaces with a moderate hydrophilicity (30−60°) have been shown to be optimal for cell adhesion, proliferation, and function.[41] Surfaces that are too hydrophilic or too hydrophobic, like PLLA, are less cytocompatible. Water contact angles of Pen-PLLAs and corresponding copolymers (undoped or doped with CSA) were determined and the results are shown in Figure 9. The water contact angles of Pen-PLLA80000, Pen-PLLA40000, and Pen-PLLA20000 are all over 80°, and they increase with increased $M_{n\text{-NMR}}$ of the PLLA branches, although the differences between them are small. The corresponding copolymers have a lower water contact angle than the pure

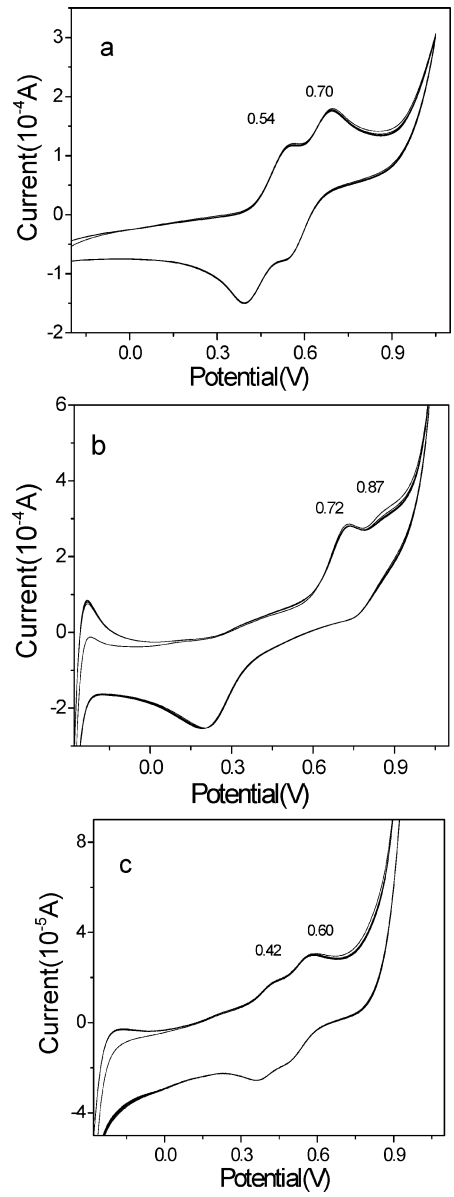

Figure 8. Cyclic voltammograms for (a) ACAT, (b) CCAT, and (c) Copo-Pen-PLLA20000 in a DMSO/HCl mixture. The scan rate was 60 mV/s.

PLLAs. This is due to more hydrophilic structure of CCAT, which contains carboxyl groups and amide groups. With a higher content of CCAT, a lower water contact angle was observed indicating a more hydrophilic surface. The decrease to 63−54° of water contact angles of copolymers doped with CSA can be explained by the formation of emeraldine salt. The same trend was also found for the linear and six-armed PLLAs and their copolymers. These intermediately hydrophilic surfaces are more suitable for cell adhesion and proliferation.

Thermal Properties of the Polymers. The T_g and T_m of the polymers determined by DSC are listed in Table 2. The T_g of linear and branched pure PLLAs and copolymers is between 48 and 58 °C, and they increase with increasing molecular weight of the PLLA segment. The T_g of the pure PLLAs is somewhat higher than that of the corresponding copolymer. This may be because, on the one hand, CCAT at the chain end of the PLLAs hinders the molecular segment movement of the PLLA chain because of the rigid configuration of CCAT, which increases the T_g of the copolymers; on the other hand, CCAT behaves as plasticizer for PLLA as it can move freely in the PLLA chain end, and this

Scheme 3. Molecular Structure of CCAT in Various Oxidation States

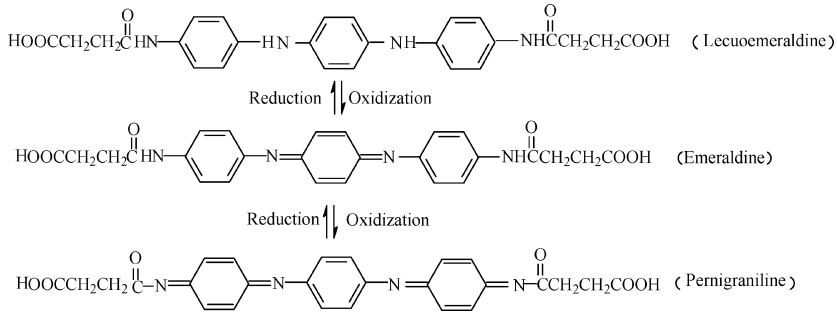

decreases the T_g of the copolymer. As a result of the two opposing effects, the T_g of the copolymers is slightly lower than that of the corresponding PLLAs. The T_g of four- and six-armed branched pure PLLAs and copolymers is less than that of their linear PLLA counterparts, because the branched molecular architecture reduces the interaction between the macromolecules.

The T_m of pure PLLA and corresponding copolymers exhibits a pattern similar to that of the T_g. T_m increases with increasing the molecular weight of PLLA, and decreases as the number of arms increases. The T_m of the pure linear and branched PLLA is from 178 to 150 °C, and the T_m of the copolymers decreases from 177 to 146 °C, depending on the molecular weight and number of arms. This is related to crystalline imperfections due to more free end groups in the more branched polymers. Figure 10 shows that the crystalline peak of Copo-Pen-PLLA20000 is at a lower temperature and has a smaller area than that of Pen-PLLA20000. This is a result of two counteracting effect of CCAT on the macromolecules. The macromolecules begin to move and organize to rearrange and crystallize at a lower temperature because of the plasticizing effect of CCAT in the copolymer, but at the same time, the movement of the molecular chain is restrained to some extent because of the rigidness of the CCAT, which impedes the crystallization process. It is clear in the figure that the plasticizing effect dominates. As a consequence of these two effects, the crystalline peak is smaller, and the T_m of the copolymer is slightly lower than that of the pure PLLA counterpart.

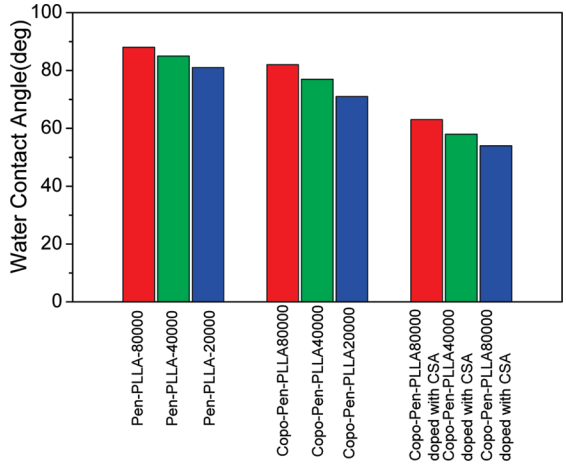

Figure 9. Water contact angle of PLLAs and corresponding undoped and doped copolymers.

Table 2. T_g and T_m of the Polymers Determined by DSC

sample code	T_g (°C)	T_m (°C)
EG-PLLA80000	58	178
EG-PLLA40000	57	172
EG-PLLA20000	53	161
Pen-PLLA80000	58	165
Pen-PLLA40000	56	156
Pen-PLLA20000	52	155
Ino-PLLA80000	55	162
Ino-PLLA40000	54	157
Ino-PLLA20000	53	150
Copo-EG-PLLA80000	58	177
Copo-EG-PLLA40000	53	172
Copo-EG-PLLA20000	49	158
Copo-Pen-PLLA80000	52	165
Copo-Pen-PLLA40000	51	154
Copo-Pen-PLLA20000	50	153
Copo-Ino-PLLA80000	52	161
Copo-Ino-PLLA40000	50	155
Copo-Ino-PLLA20000	48	146

Thermal stability of the polymer is also important for the application of electroactive polymers in many fields. To test the thermal stability of the copolymers prepared, Copo-Pen-PLLA80000, Copo-Pen-PLLA40000, Copo-Pen-PLLA20000, and Pen-PLLA20000 were tested by TGA, and the results are plotted in Figure 11. When the temperature was raised to 100−200 °C, there was a small weight loss from the PLLA and copolymers. This is attributed to water evaporation and to the loss of other solvent trapped in the copolymer. In case of pure PPLA, there was a major weight loss between 280 and 310 °C, and the residual weight above 310 °C was almost zero, indicating a degradation of the PLLA main chain. In the copolymers, the first evident weight loss occurred between 320 and 360 °C, and 80∼90% of the weight of the copolymer was lost depending on the CCAT content, due to the PLLA main chain degradation. The thermal stability of the copolymer was higher than that of the corresponding pure PLLA, due presumably to the better thermal stability of CCAT. Between 360 and 600 °C, there was another obvious weight loss of the copolymers, presumably related to the degradation of the CCAT segment. All these results indicate that the copolymer has a better thermal stability. It is also found that the stability is

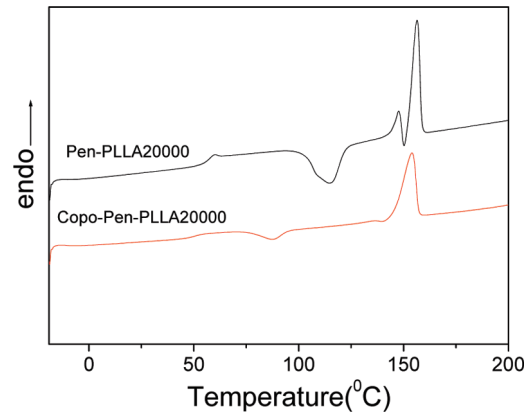

Figure 10. DSC traces of Pen-PLLA20000 and Copo-Pen-PLLA20000.

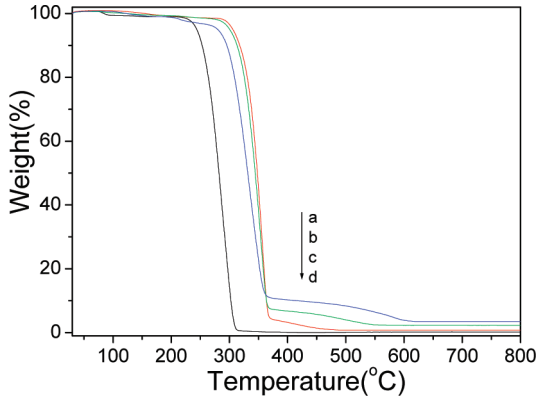

Figure 11. TGA curves of (a) Copo-Pen-PLLA20000, (b) Copo-Pen-PLLA40000, (c) Copo-Pen-PLLA80000, and (d) Pen-PLLA20000.

affected by the molecular weight, the higher the molecular weight of the copolymer, the better is the thermal stability at 320−360 °C. The residual weight of the copolymer after 600 °C was greater the higher the CCAT content in the copolymer. This also confirms the successful synthesis of the copolymers.

Conclusions

A series of branched electroactive and biodegradable copolymers was synthesized from PLLAs and CCAT. The CCAT was synthesized and its structure was verified by FT-IR and NMR. It has good electroactive property, similar to those of polyaniline. This monomer can be incorporated into a copolymer because it has carboxyl groups. It has good hydrophilic properties as it contains both carboxyl and amide groups, and it is suitable for cell adhesion and proliferation in biomedical application. Two-, four-, and six-armed star-shaped PLLAs with low organic metal residues and different molecular weights were synthesized by ROP. The copolymers consisting of PLLAs and CCAT have good electroactive properties, indicated by their CV and UV spectra. DSC and TGA studies showed a good thermal stability of the copolymers. The hydrophilicity of the copolymer film surface increased with increasing content of CCAT in the copolymer, and the water contact angle decreased dramatically to 54−63° after doping with CSA. The copolymers also have good processability as they dissolve in most organic solvents. These copolymers with different architectures can be used to tailor the thermal properties, degradation properties and surface properties to give materials that are favorable for the growth of electrically excitable cells in tissue engineering.

Acknowledgment. The authors thank the Swedish Research Council (Grant No. 2008-5538), China Scholarship Council and The Royal Institute of Technology (KTH) for financial support of this work. The assistance of Assoc. Prof. Ann Maria Cornell and M.Sc. Simon Leijonmarck for cyclic voltammetry measurements is gratefully acknowledged.

Supporting Information Available. ^{1}H NMR and CVs of the two- and six-armed copolymers. This material is available free of charge via the Internet at http://pubs.acs.org.

References and Notes

(1) Wong, J. Y.; Langer, R.; Ingber, D. E. *Proc. Natl. Acad. Sci. U.S.A.* **1994**, *91*, 3201–3204.
(2) Jiang, X. P.; Marois, Y.; Traore, A.; Tessier, D.; Dao, L. H.; Guidoin, R.; Zhang, Z. *Tissue Eng.* **2002**, *8*, 635–647.
(3) Schmidt, C. E.; Shastri, V. R.; Vacanti, J. P.; Langer, R. *Proc. Natl. Acad. Sci. U.S.A.* **1997**, *94*, 8948–8953.
(4) Guimard, N. K.; Gomez, N.; Schmidt, C. E. *Prog. Polym. Sci.* **2007**, *32*, 876–921.
(5) Cui, X. Y.; Wiler, J.; Dzaman, M.; Altschuler, R. A.; Martin, D. C. *Biomaterials* **2003**, *24*, 777–787.
(6) Kang, E. T.; Neoh, K. G.; Huang, S. W.; Lim, S. L.; Tan, K. L. *J. Phys. Chem. B* **1997**, *101*, 10744–10750.
(7) Li, M. Y.; Guo, Y.; Wei, Y.; MacDiarmid, A. G.; Lelkes, P. I. *Biomaterials* **2006**, *27*, 2705–2715.
(8) Ho, H. A.; Boissinot, M.; Bergeron, M. G.; Corbeil, G.; Dore, K.; Boudreau, D.; Leclerc, M. *Angew. Chem., Int. Ed.* **2002**, *41*, 1548–1551.
(9) Zhang, L. P.; Peng, H.; Kilmartin, P. A.; Soeller, C.; Travas-Sejdic, J. *Macromolecules* **2008**, *41*, 7671–7678.
(10) Wang, C. H.; Dong, Y. Q.; Sengothi, K.; Tan, K. L.; Kang, E. T. *Synth. Met.* **1999**, *102*, 1313–1314.
(11) Li, Y. L.; Neoh, K. G.; Cen, L.; Kang, E. T. *Biotechnol. Bioeng.* **2003**, *84*, 305–313.
(12) Hu, J.; Huang, L. H.; Zhuang, X. L.; Chen, X. S.; Wei, Y.; Jing, X. B. *J. Polym. Sci., Part A: Polym. Chem.* **2008**, *46*, 1124–1135.
(13) Wan, Y.; Wu, H.; Wen, D. J. *Macromol. Biosci.* **2004**, *4*, 882–890.
(14) Piza, M. A.; Constantino, C. J. L.; Venancio, E. C.; Mattoso, L. H. C. *Polymer* **2003**, *44*, 5663–5670.
(15) Chen, Y. J.; Kang, E. T.; Neoh, K. G.; Wang, P.; Tan, K. L. *Synth. Met.* **2000**, *110*, 47–55.
(16) Shi, G. X.; Rouabhia, M.; Wang, Z. X.; Dao, L. H.; Zhang, Z. *Biomaterials* **2004**, *25*, 2477–2488.
(17) Shi, G. X.; Zhang, Z.; Rouabhia, M. *Biomaterials* **2008**, *29*, 3792–3798.
(18) Sanghvi, A. B.; Miller, K. P. H.; Belcher, A. M.; Schmidt, C. E. *Nat. Mater.* **2005**, *4*, 496–502.
(19) Korri-Youssoufi, H.; Yassar, A. *Biomacromolecules* **2001**, *2*, 58–64.
(20) Zelikin, A. N.; Lynn, D. M.; Farhadi, J.; Martin, I.; Shastri, V.; Langer, R. *Angew. Chem., Int. Ed.* **2002**, *41*, 141–144.
(21) Rivers, T. J.; Hudson, T. W.; Schmidt, C. E. *Adv. Funct. Mater.* **2002**, *12*, 33–37.
(22) Guimard, N. K. E.; Sessler, J. L.; Schmidt, C. E. *Macromolecules* **2009**, *42*, 502–511.
(23) Huang, L. H.; Hu, J.; Lang, L.; Wang, X.; Zhang, P. B.; Jing, X. B.; Wang, X. H.; Chen, X. S.; Lelkes, P. I.; MacDiarmid, A. G.; Wei, Y. *Biomaterials* **2007**, *28*, 1741–1751.
(24) Huang, L. H.; Zhuang, X. L.; Hu, J.; Lang, L.; Zhang, P. B.; Wang, Y. S.; Chen, X. S.; Wei, Y.; Jing, X. B. *Biomacromolecules* **2008**, *9*, 850–858.
(25) Ding, C. F.; Wang, Y.; Zhang, S. S. *Eur. Polym. J.* **2007**, *43*, 4244–4252.
(26) Lu, W.; Meng, X. S.; Wang, Z. Y. *J. Polym. Sci., Part A: Polym. Chem.* **1999**, *37*, 4295–4301.
(27) Wang, Z. Y.; Yang, C.; Gao, J. P.; Lin, J.; Meng, X. S.; Wei, Y.; Li, S. *Macromolecules* **1998**, *31*, 2702–2704.
(28) Rebourt, E.; Joule, J. A.; Monkman, A. P. *Synth. Met.* **1997**, *84*, 65–66.
(29) Guo, Y.; Li, M. Y.; Mylonakis, A.; Han, J. J.; MacDiarmid, A. G.; Chen, X. S.; Lelkes, P. I.; Wei, Y. *Biomacromolecules* **2007**, *8*, 3025–3034.
(30) Finne, A.; Albertsson, A.-C. *Biomacromolecules* **2002**, *3*, 684–690.
(31) Finne, A.; Albertsson, A.-C. *J. Polym. Sci., Part A: Polym. Chem.* **2004**, *42*, 444–452.
(32) Numata, K.; Srivastava, R. K.; Finne-Wistrand, A.; Albertsson, A.-C.; Doi, Y.; Abe, H. *Biomacromolecules* **2007**, *8*, 3115–3125.
(33) Odelius, K.; Finne, A.; Albertsson, A.-C. *J. Polym. Sci., Part A: Polym. Chem.* **2006**, *44*, 596–605.
(34) Andronova, N.; Albertsson, A.-C. *Biomacromolecules* **2006**, *7*, 1489–1495.
(35) Hakkarainen, M.; Hoglund, A.; Odelius, K.; Albertsson, A.-C. *J. Am. Chem. Soc.* **2007**, *129*, 6308–6312.
(36) Wei, Y.; Yang, C. C.; Ding, T. Z. *Tetrahedron Lett.* **1996**, *37*, 731–734.
(37) Stjerndahl, A.; Wistrand, A. F.; Albertsson, A.-C. *Biomacromolecules* **2007**, *8*, 937–940.
(38) Stejskal, J.; Kratochvil, P.; Radhakrishnan, N. *Synth. Met.* **1993**, *61*, 225–231.
(39) Guo, Y.; Mylonakis, A.; Zhang, Z. T.; Lelkes, P. I.; Levon, K.; Li, S. X.; Feng, Q. W.; Wei, Y. *Macromolecules* **2007**, *40*, 2721–2729.
(40) Bhadani, S. N.; Gupta, M. K.; Sengupta, S. K. *J. Appl. Polym. Sci.* **1993**, *49*, 397–403.
(41) Andrade, J. D.; King, R. N.; Gregonis, D. E.; Coleman, D. L. *J. Polym. Sci., Polym. Symp.* **1979**, 313–336.

BM9011248